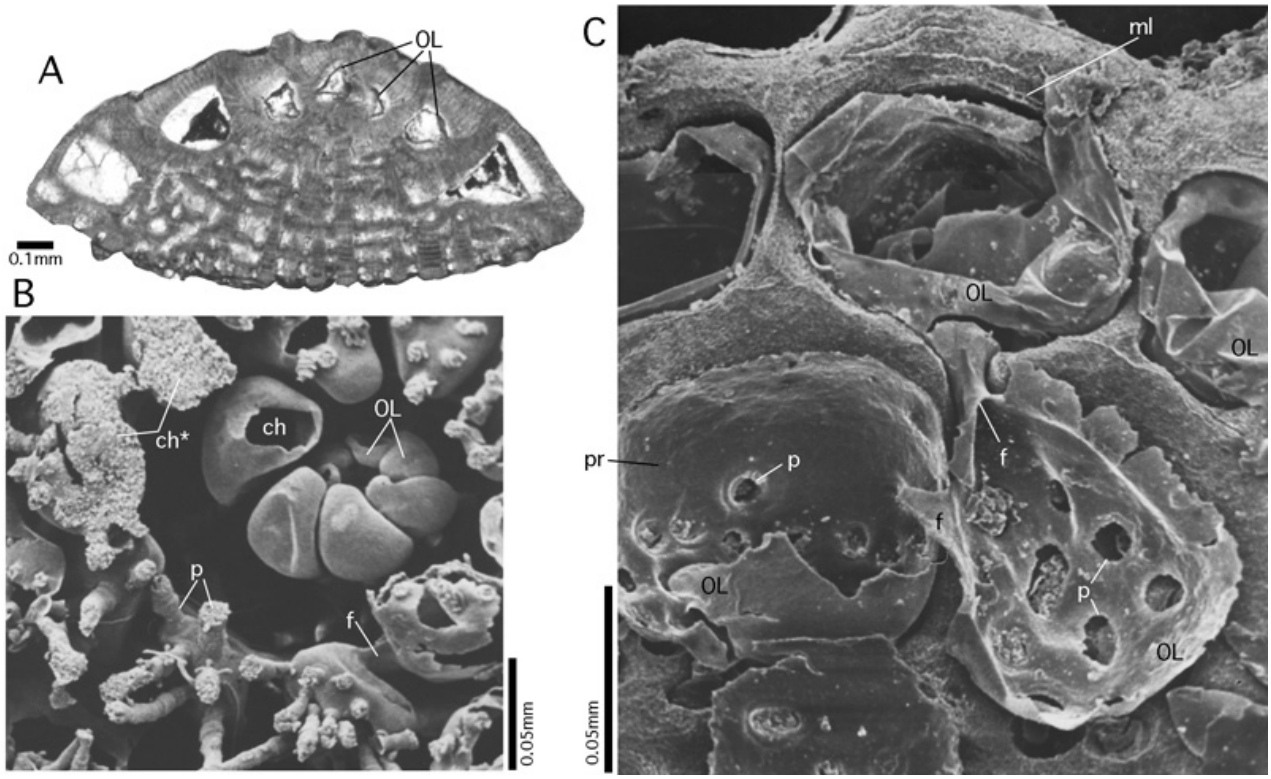

Figure 69: Organic lining.
A: *Lockhartia haimei* (DAVIES), megalospheric specimen, axial section, transmitted light micrograph. From the Salt Range, Pakistan. Paleocene. Note the detachment of the organic lining from the inner surface of the biomineralized chamber wall by the first generation of cement deposited during early diagenesis. **B-C:** *Planorbulinella larvata* (PARKER et JONES). Gulf of Aqaba, Red Sea; Recent. **B:** SEM graph of epoxy resin cast of a microspheric specimen. The subequatorial section of the shell reveals the detail of the early stages of growth, where the resin could not penetrate into the nepionic spiral chambers. After the dissolution of the mineralized shell, the organic lining alone documents the earliest chambers. **C:** megalospheric specimen, equatorial section, etched in order to reveal the organic lining and the lamellation of the chamber walls. The drying of the preparation before its coating for the SEM contracted the organic lining, detached it from the inner surface of the mineralized wall and broke the connection with the organic poreplugs at their weakest spot. This produced the circular holes in the organic lining of the preparation. Note the organic lining that coats the foramina connecting the first three chambers.
ch: chamber; **ch*:** late spiral chamber filled with epoxy resin; **f:** foramen; **ml:** median layer of the primary chamber wall separating the inner from all outer lamellae; **OL:** organic lining; **p:** pore.

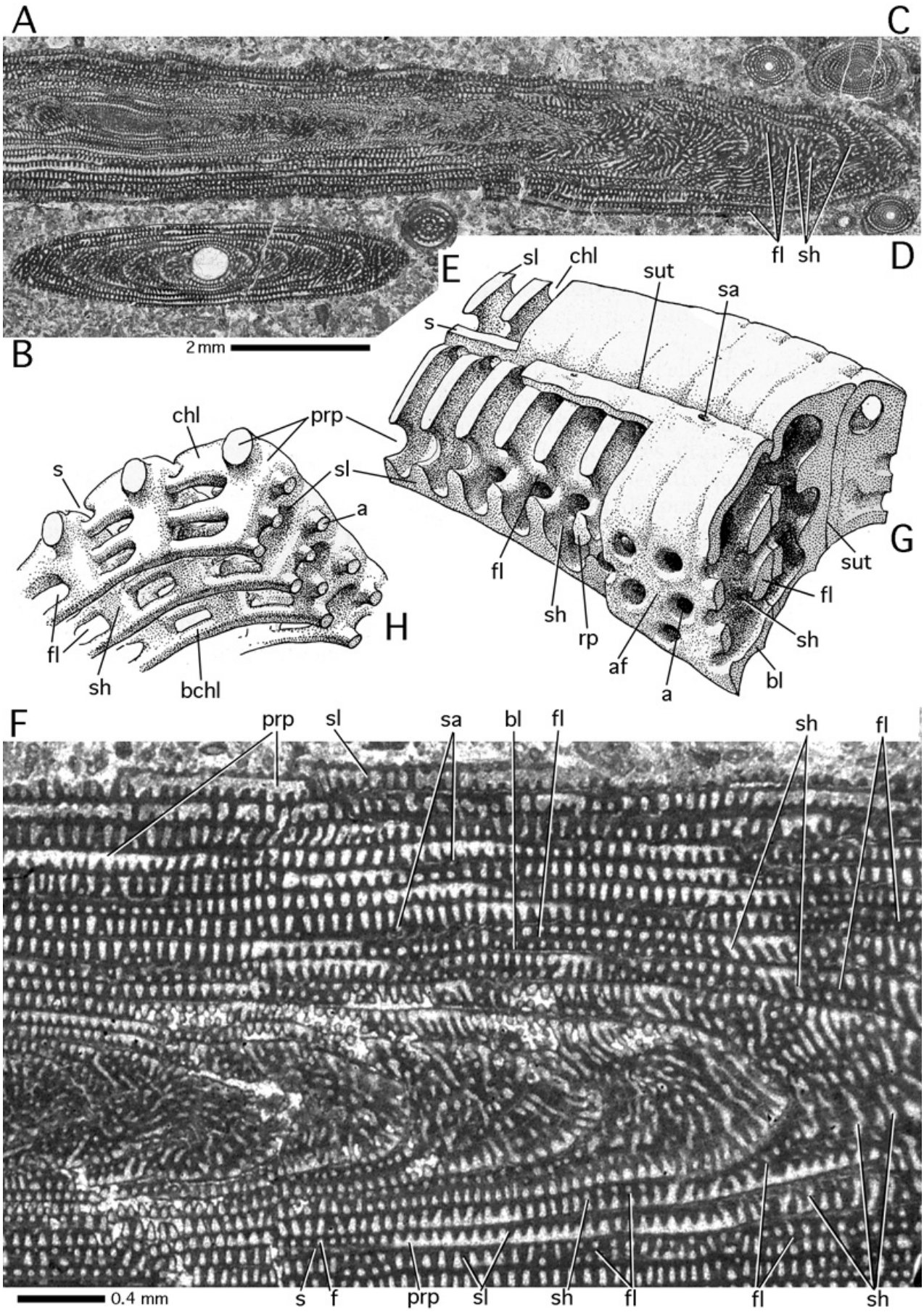
A
C
fl
sh
D
B
2 mm
E
sl
chl
sut
sa
s
G
fl
sh
rp
af
a
bl
sut
fl
sh
chl
prp
s
sl
a
fl
sh
bchl
H
F
prp
sl
sa
bl
fl
sh
fl
0.4 mm
s
f
prp
sl
sh
fl
fl
sh

◀ **Figure 70:** Odd association and polar structures in *Praealveolina tenuis* REICHEL. From Alcantara, Lisbon; Cenomanian. Transmitted light micrographs.
A: microspheric specimen, axial section; **B:** megalospheric specimen, axial section; **C-E:** odd partners: **C:** axial section of microspheric *Simplalveolina* sp.; **D:** axial sections of megalospheric *Simplalveolina* sp.; **E:** *Ovalveolina* sp, axial section. **F:** microspheric *P. tenuis*, axial section, detail showing polar structure with floors and shaftsin the basement. **G:** model of two subsequent chambers near their polar ends where the first floors in the basement appear. **H:** model of the protoplasmic body filling the cavities in G. Both models schematic, not to scale, after REICHEL, 1933.
a: aperture: **af:** apertural face; **bchl:** basement chamberlets; **bl:** basal layer; **chl:** (main) chamberlets; **fl:** floor; **prp:** preseptal passage; **rp:** (incipient) residual pillar; **s:** septum; **sa:** supplementary aperture; **sh:** shaft; **sl:** septulum; **sut:** cameral suture.

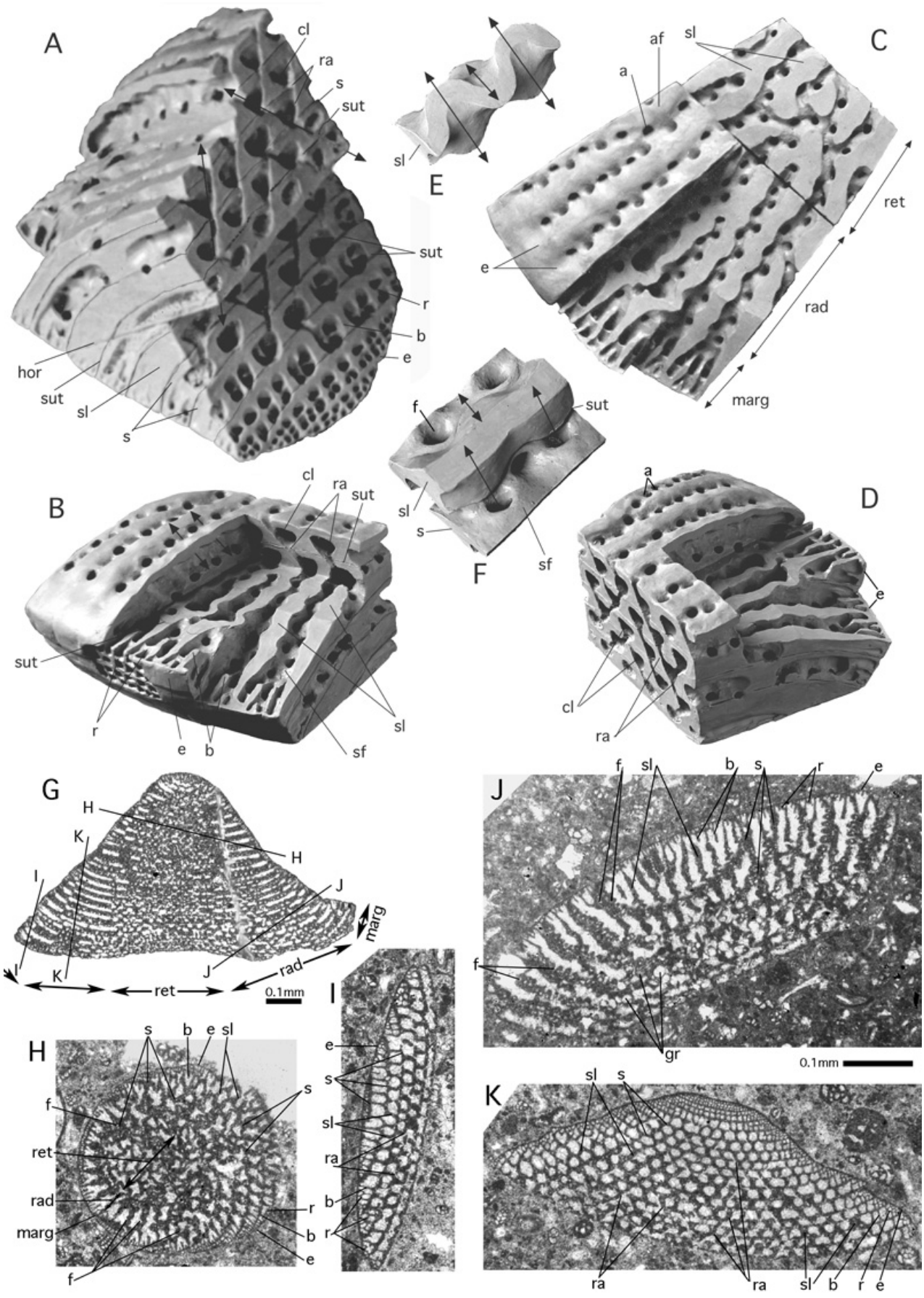
A
cl
ra
s
sut
sut
r
b
e
hor
sut
sl
s
E
sl
C
af
a
sl
ret
e
rad
marg
f
sut
sl
s
sf
F
B
cl
ra
sut
sut
r
e
b
sl
sf
D
a
e
cl
ra
G
H
K
I
H
J
I
K
J
marg
rad
ret
0.1mm
J
f
sl
b
s
r
e
f
gr
0.1mm
H
s
b
e
sl
f
s
ret
rad
r
marg
b
e
f
I
e
s
sl
ra
b
r
K
sl
s
ra
ra
sl
b
r
e

◀ **Figure 71:** The structure of *Orbitolina*.
A-D: Oblique and vertical views of the cone base. These plasticine models sculptured in the years around 1955 by M. REICHEL (* 1896 - † 1984) were never published. **E-F:** Details of a septulum in the radial zone of the discoidal chamber. In model E the septulum is cut below the roof and above the bottom of the chambers. The apparent folding of the section results from the adjustment of the endoskeletal structure to the crosswise-oblique arrangement of the stolon axes (arrows) that produce so-called ramps. In model F the septulum is cut in the middle of the chamber and shows a part of the chamber bottom with the face of the previous chamber. In the middle of the chamber, the section of the septulum appears unfolded. Compare Fig. 47H and Fig. 80G. **G-H:** Random thinsections of *Orbitolina* sp. from Southwestern France, Albian. Transmitted light micrographs. In Fig. G the approximate positions of sections H-K are indicated. Note the inverse orientation: the sections face downward. **G-K:** Random sections of *Orbitolina* sp. from Southwestern France, Albian. Transmitted light micrographs. The approximate position of sections H-K are indicated in section G that is very close to the axial plane. For HENSON's zonation of the chamber see Fig. 20. Section H demonstrates details of the reticular zone, section I details of the marginal zone and section J details of the radial zone. The transverse section K shows the ramps produced by the crosswise-oblique stolon system.
a: aperture; **af:** apertural face; **b:** beam; **cl:** chamberlet; **e:** epiderm; **f:** foramen; **gr:** coarse grains in the septum that obscure the structural pattern; **hor:** horizontal section in the plasticine model; **marg:** marginal zone; **r:** rafter; **ra:** ramp; **rad:** radial zone; **ret:** reticular zone; **s:** septum; **sf:** septal face; **sl:** septulum; **sut:** suture of the chambers. Double arrows in E and F: crosswise oblique foraminal axes.

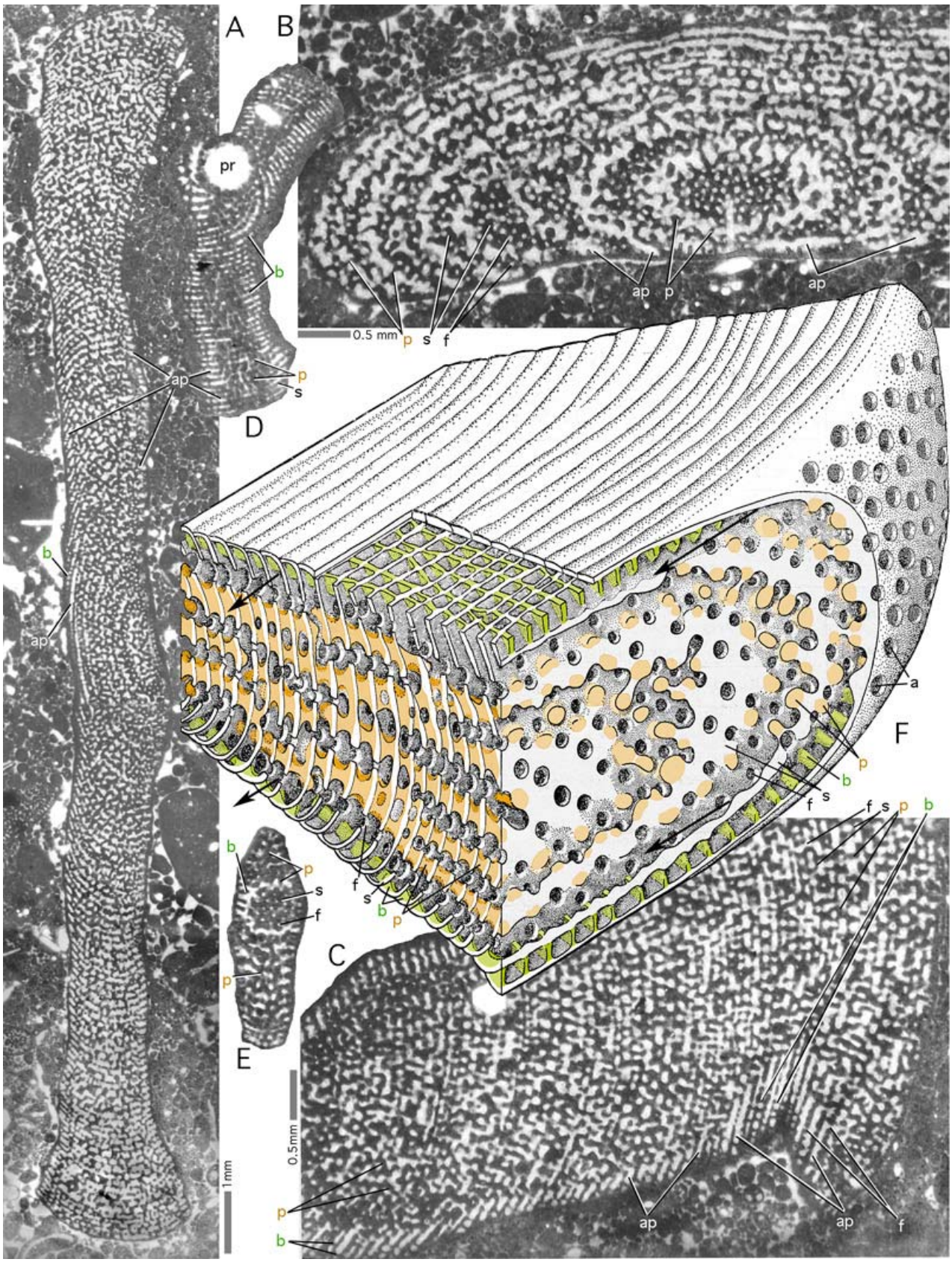
A
B
pr
b
ap
p
s
f
0.5 mm
D
a
F
C
E
1 mm
0.5mm

◀ **Figure 72:** The structure of *Orbitopsella*: a simple exoskeleton and a pillared endoskeleton in a discoidal shell: *Orbitopsella dubari* HOTTINGER, Bou Dahar, Eastern Morocco, Middle Lias. Transmitted light micrographs.
A: oblique section of complete microspheric specimen; **B:** oblique section of microspheric specimen. The septa of the thickened margin are cut tangentially and reveal the alternating pattern in the disposition of foramina on the septal face. **C:** oblique tangential section of a microspheric specimen at a low angle to the equatorial plane showing a part of the disc with its exoskeleton (restricted to beams). Note the large open spaces, the lateral annular passages (**arrows**), that separate exoskeleton and endoskeleton. **D:** Oblique centered section of megalospheric specimen. Note the structured wall of the embryo, that shows it to be a sphaeroconch. **E:** Transverse section (parallel to the axis of coiling) of a megalospheric specimen. The septum in this tangential section reveals the alternating pattern of the apertures. **F:** schematic model of structure after HOTTINGER, 1967; not to scale.
Green: exoskeleton; **brown:** endoskeleton.
a: aperture; **ap:** annular passage; **b:** beam; **f:** foramen; **p:** pillar; **pr:** sphaeroconch; **s:** septum.

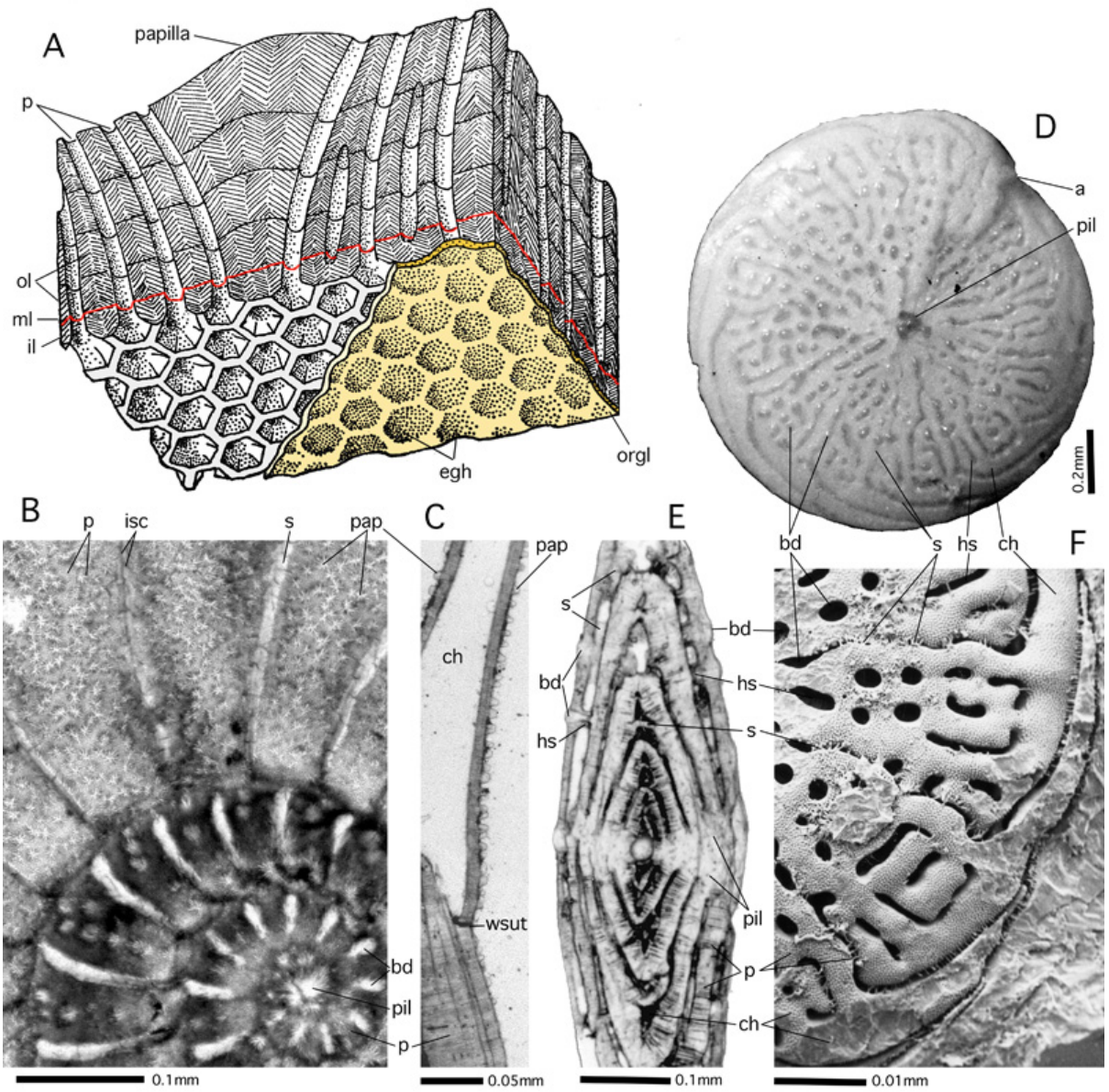

Figure 73: Papillae, beads and axial piles of lamellae.
A: papilla and pores. Stereograph, schematic, not to scale; after HOTTINGER, 1977. **B-C:** *Assilina madagascariensis* (d'ORBIGNY) from Mauritius. Recent. Transverse section parallel to equatorial plane (B) and axial section (C) with minute papillae on the last whorl; transmitted light micrograph. **D-F:** Beading in *Amphistegina papillosa* SAID. Gulf of Aqaba, Red Sea; Recent. **D:** dorsal view of shell showing beading of septular and hemiseptular sutures. Incident light micrograph. **E:** axial section showing hemiseptular and septular support of beads; transmitted light micrograph. **F:** Epoxy resin cast of shell cavity showing spiral main chamber lumina in dorsal view, interrupted by the hemiseptula supporting the interseptal beads, SEM graph.
a: aperture; **bd:** beads (septular and hemiseptular); **ch:** main (spiral) chamber lumen; **egh:** eggholders; **hs:** hemiseptulum; **il:** inner lamella; **isc:** intraseptal canal system; **ml:** median layer; **ol:** outer lamellae; **orgl:** organic lining of protoplast; **p:** pores; **pap:** papillae; **pil:** axial pile of lamellae; **s:** septum and septal suture; **wsut:** whorl suture.

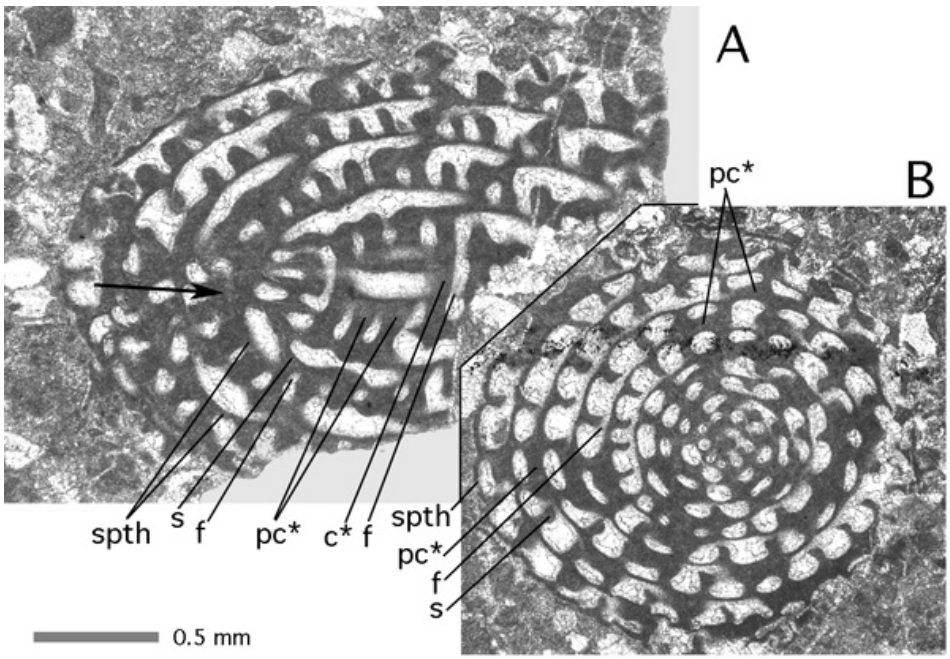

Figure 74: Parachomata in *Pseudodoliolina* sp. from a commercial thin section labeled "Moscow", Permian.
A: oblique section at low angle to axis of coiling (arrow). **B:** oblique section nearly perpendicular to the axis of coiling.
c*: choma; **f:** foramina forming a single row in alternation with the parachomata; **s:** septum (without fluting); **spth:** spirotheca (no trace of keriotheca).

Figure 75: The pore and its organic constituents. ▶
A: a pore in an inner chamber covered by an outer whorl, according to LEUTENEGGER (1977), schematic, not to scale. **B:** Accumulation of mitochondria below a pore mouth in *Bolivina* sp., thus indicating the pores' main function: gas exchange. TEM micrograph of a section oblique to the surface ot the wall that exaggerates the thickness of the pore discs. The detachment of the outer lamella 2 (ouL 2) is an artifact of preparation. x 22,700. Courtesy S. REBER-LEUTENEGGER. **C:** Resin cast of pores in the lateral chamber wall of *Nummulites partschi* DE LA HARPE with trabeculae. The carbonates of the shell are dissolved with HCl. SEM graph x 950. **D:** Outer pore mouths in the lateral suface of chamber wall of *Assilina*. Note the annular attachment of the interlamellar discs. SEM graph x4,700. **E:** Inner pore mouths in the lateral chamber wall of *Assilina* shaped as eggholders (in order to keep the symbionts below their breathing chimneys). Note the annular suture of the pore plug. SEM graph x 4,700. C-E from HOTTINGER, 1977. **F:** Perforation pattern on the dorsal surface of *Challengerella persica* (Recent, Persian Gulf): densely perforated porefields between imperforate ornamentation. SEM: oblique dorsal view of shell, x 28, and detail of porefield, x 470. **G:** Perforation pattern in *Ammonia reyi* MARIE (Pliocene, Dar bel Hamri, Northern Morocco): densely perforated porefields between loosely perforated ornaments. SEM graphs of dorsal shell view (x 28) with detail (x 470). **F-G:** from BILLMAN *et alii*, 1980.
Abbreviations: **bD:** basal (pore) disc; **Cy:** cytoplasm; **iL:** inner lamella; **iID:** interlamellar disc; **iol:** interlamellar organic lining; **ls:** lacunar system (in the cytoplasm); **M:** mitochondria; **ML:** median layer separating inner from outer lamellas; **OL:** Organic lining (here difficult to separate from plasmalemma of host); **ouL 1:** primary outer lamella; **ouL 2, 3:** subsequent outer lamellas; **P:** pore; **Pc:** organic pore coat; **Pl:** plasmalemma; **ppl:** pore plug (note its porosity); **Spl:** (biomineralized) sieveplate; **V:** vacuole.

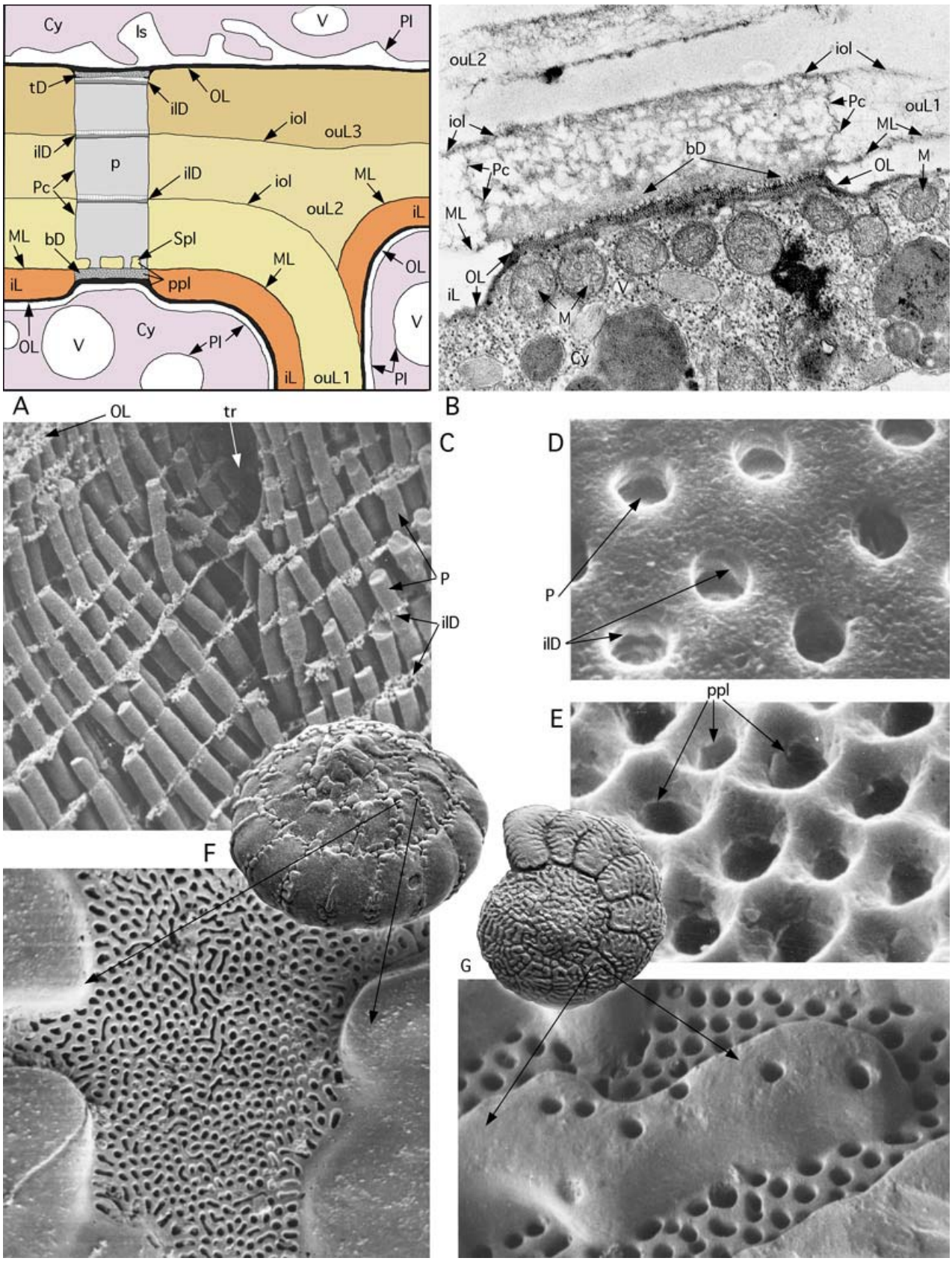
Cy
ls
V
Pl
tD
ilD
OL
iol
ouL3
p
Pc
ML
bD
Spl
ppl
iL
ouL2
ouL1
A
B
C
D
E
F
G
tr
P

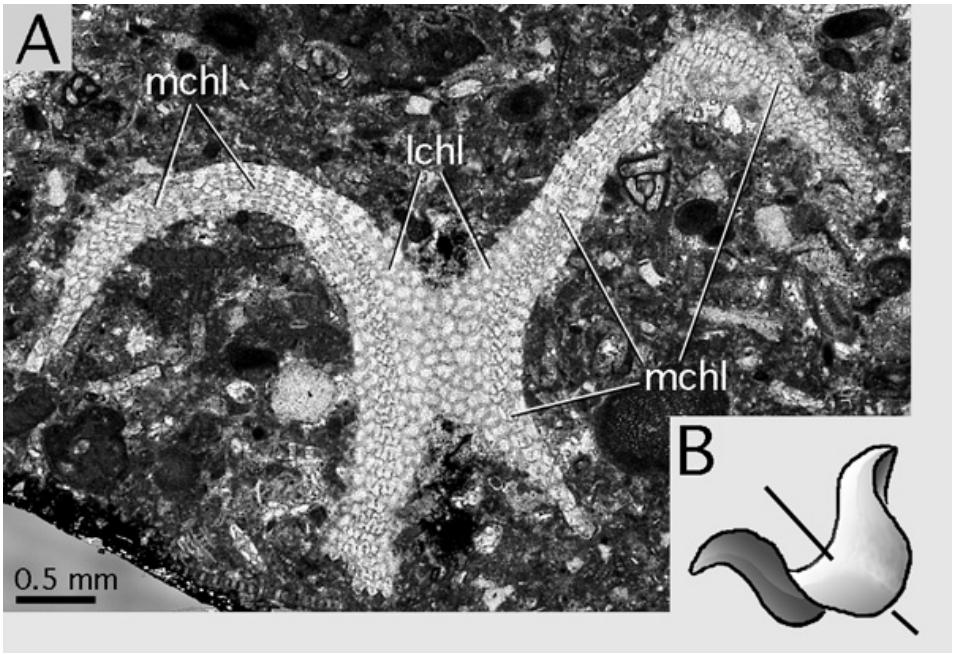

Figure 76: A: selliform deformation of the lenticular-compressed test of *Eulepidina* sp., Oligocene, Sarawak, Borneo. Transverse section approximately perpendicular to the axis of the shell. Transmitted light micrograph. **B:** sketch of a selliform shell with its axis. Schema, not to scale.

Figure 77: Umbos and umbilical plugs. ▶
A-C: *Elphidium craticulatum* (FICHTEL et MOLL) from the Gulf of Aqaba, Red Sea. Recent. **A:** lateral view, SEM graph. **B:** peripheral view, SEM graph. **C:** slightly oblique axial section cutting through the symmetrical pair of umbilical plugs. Note the presence of spaces in the biumbilical shell, caused by spiral canals and funnels. Transmitted light micrograph. **D-E:** *Amphistegina lessonii* d'ORBIGNY from the Gulf of Aqaba, Red Sea. Recent. **D:** ventral view shows the stellar chamberlets overgrowing part of the ventral umbo. Incident light micrograph. **E:** axial section of specimen having lost the last few chambers. There is a smaller dorsal and a larger ventral umbo. **F-G:** *Ammonia umbonata* (LEROY). Dorsal and ventral views, SEM graphs. The ventral (umbilical) view exhibits a free-standing, composite umbilical plug. **H-I:** the umbos in porcelaneous shells may react to diagenetic processes by differences in recrystallisation that possibly indicate a differentiation in the texture of the wall in the umbonal area of the shell. Diagnostic for the involute stages in the growth of Meandropsinidae in the Upper Cretaceous of the Pyrenean Gulf. **H:** megalospheric *Fascispira* sp. from Canelles, Lerida, Northern Spain. Axial section. **I:** microspheric *Larrazetia larrazeti* (SCHLUMBERGER), center of axial section, from Bac de Grillera, Northern Spain. All scale bars 0.1 mm.
a: aperture; **af:** apertural face; **cpl:** coverplate; **f:** foramen; **fo:** fossette; **fpl:** foramenal plate; **fu:** funnel; **k:** keel; **m:** mask; **pust:** pustules on amphisteginid face; **rp:** retral process; **s:** septum; **spc:** spiral canal; **ub:** umbo; **up:** umbilical plate; **upl:** umbilical plug.

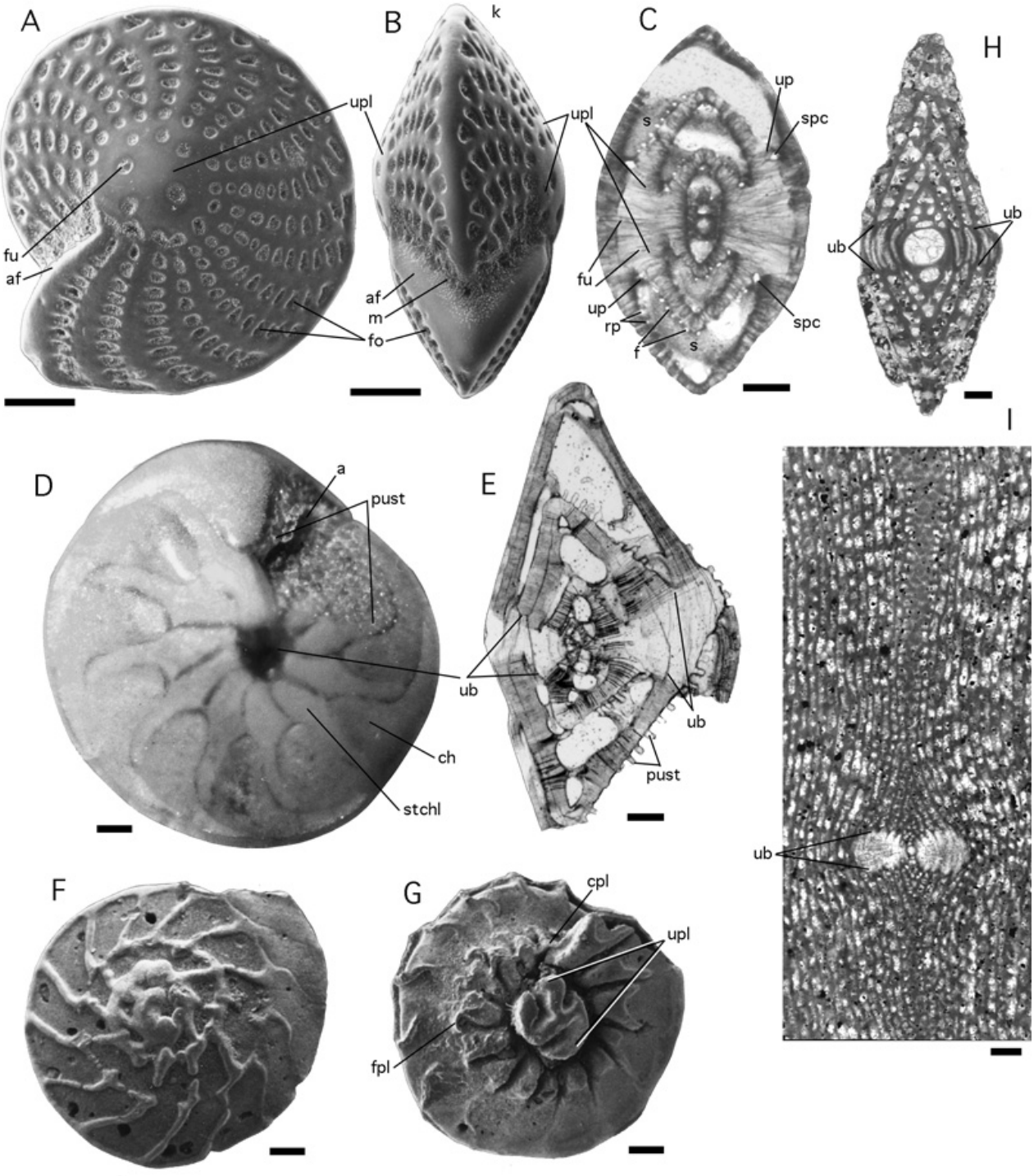
A
upl
fu
af
fo
B
k
upl
af
m
fo
C
up
spc
s
upl
fu
up
rp
f
s
spc
H
ub
ub
ub
I
ub
D
a
pust
ub
ch
stchl
E
ub
ub
pust
F
G
cpl
upl
fpl

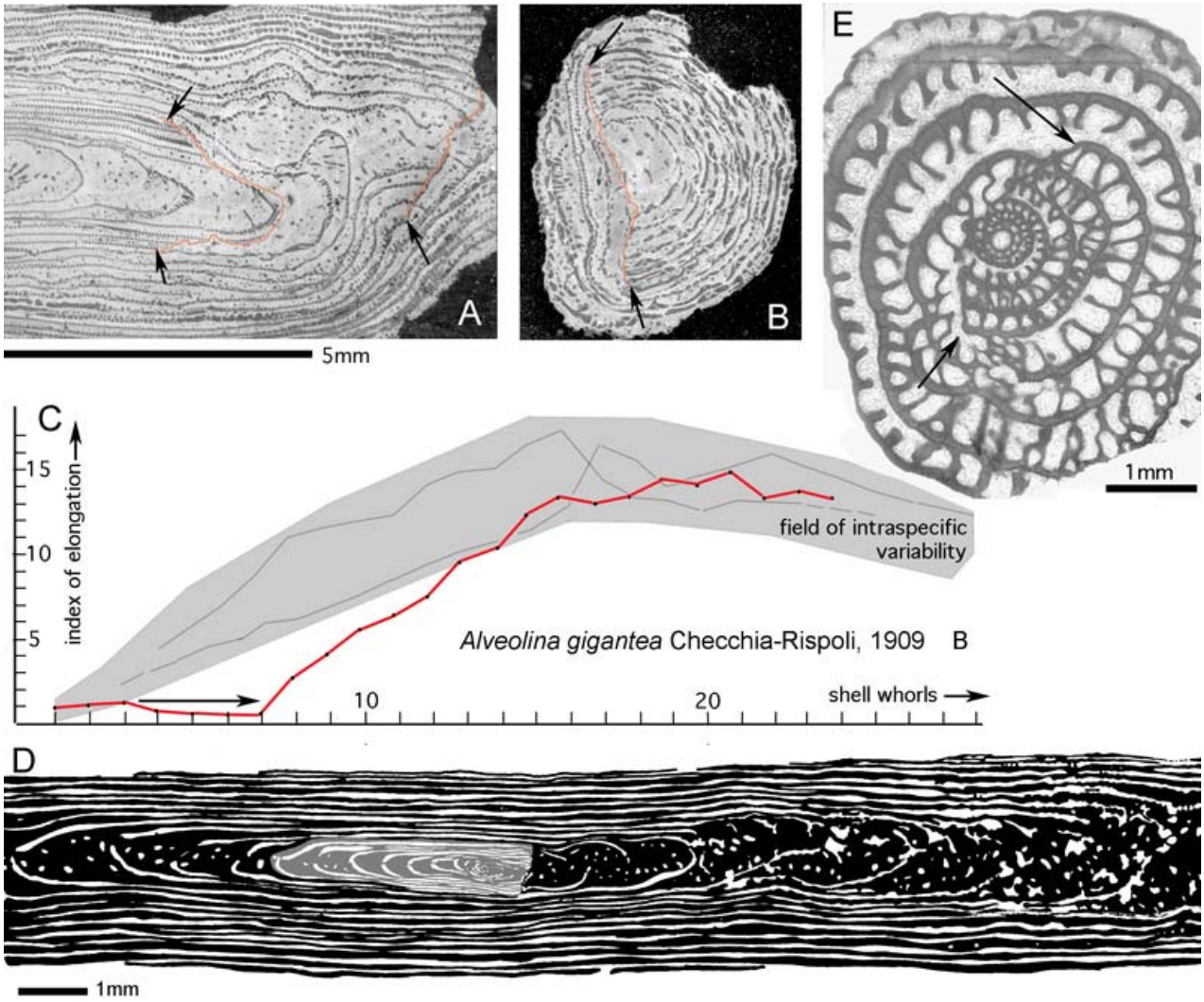

Figure 78: Regeneration in fusiform-elongate shells: **A-D:** *Alveolina gigantea* CHECCHIA-RISPOLI. Microspheric generation. Palermo, Sicily, Middle Eocene. **E:** *Pseudoschwagerina* sp., megalospheric specimen, from Palazzo Adriano, Sicily, Permian.
A: a fragment of the polar realm of the shell cut in the axial direction shows two periods of regeneration (red lines designated by arrows) during late ontogeny. **B:** a similar fragment cut in a direction perpendicular to the shell axis, with one broken surface, that has been regenerated in an attempt to restore the cylindrical shape of the shell. At such a late ontogenetic stage the original shape of the shell can not be regained through regenerative growth. Incident light micrographs. **C-D:** regeneration at an early stage of ontogeny: **C.** the rate of elongation was higher in the regenerated half of the shell (red curve) than in the undisturbed half, until the range of elongation that is characteristic for the species was attained again. Note the absence of elongation index increase in the early whorls broken away (arrow). Data from HOTTINGER, 1962. **D.** Compare the camera lucida drawing of an axial section: broken early shell in gray, regenerated shell in black. **E:** in a fusulinid the regeneration of the broken whorls 3-6 produces an almost perfect equatorial spiral after only two more whorls of growth.

Figure 79: Preseptal (**prp**) and postseptal (**pop**) passages. ▶
A: *Alveolina munieri* HOTTINGER (equatorial section of microspheric specimen, Middle Lutetian, S. Giovanni Ilarione, Northern Italy). **B-E:** unpublished plasticine models of the shell by M. REICHEL. **B-C:** oblique views showing chamberlets. In **C** the chamber roof (spirotheca) is partly removed. **D:** side view of chamber showing septum and passages behind and in front of it. **E:** oblique view complementary to B showing main and intercalary apertures. the septal realm between two adjacent chambers. **F-H:** unpublished models of sarcode (=shell cavities) by M. REICHEL seen from above (F), obliquely from the side (G) and from below (H); **Arrows:** direction of growth.
bl: basal layer; **chl:** chamberlet; **chlsut:** chamberlet suture; **chsut:** chamber suture; **f:** foramen; **icf:** intercalary foramen; **pop:** postseptal passage; **prp:** preseptal passage; **prwsurf:** chamber roof surface of previous whorl; **s:** septum; **sl:** septulum; **sup:** supplementary passages in basal layer; **sut:** suture (of chambers); **te:** chamber roof (tectum).

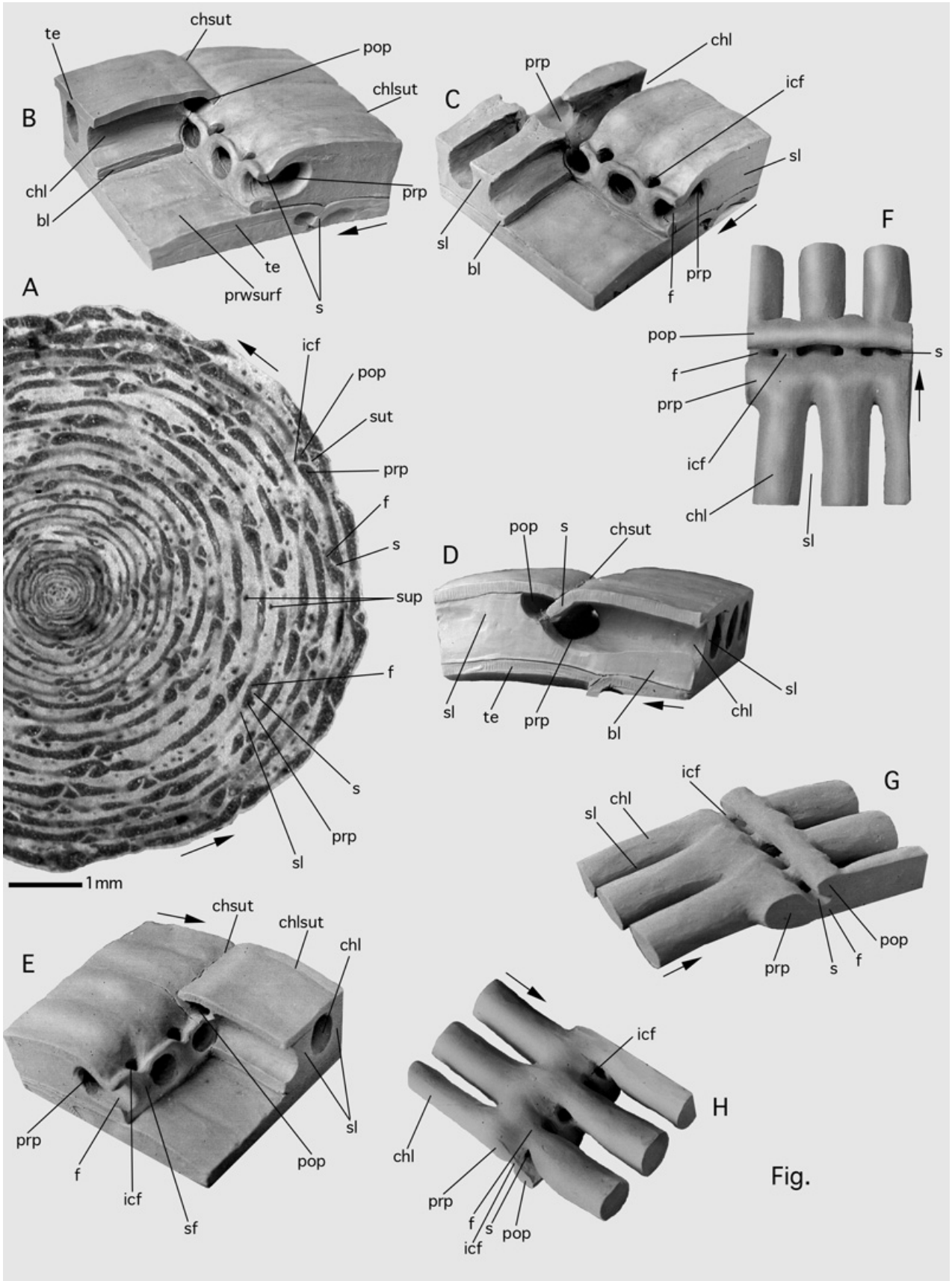
B
te
chsut
pop
chlsut
chl
bl
prp
te
prwsurf
s
C
prp
chl
icf
sl
sl
bl
prp
f
F
pop
s
f
prp
icf
chl
sl
A
icf
pop
sut
prp
f
s
sup
f
s
prp
sl
1mm
D
pop
s
chsut
sl
sl
te
prp
bl
chl
G
icf
chl
sl
pop
prp
s
f
E
chsut
chlsut
chl
prp
f
icf
sf
pop
sl
H
icf
chl
prp
f
s
pop
icf

Fig.

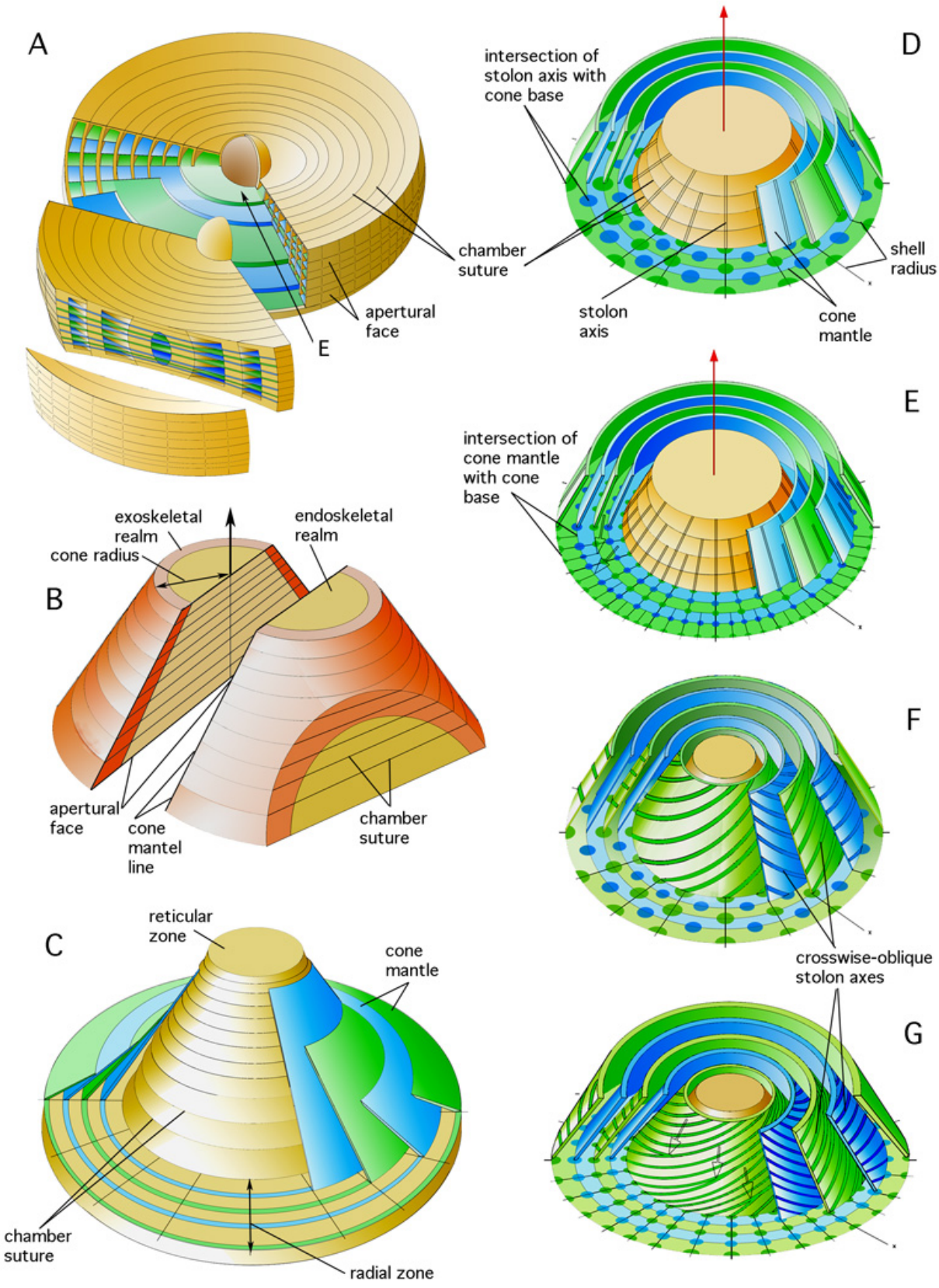
A
chamber suture
apertural face
E
D
intersection of stolon axis with cone base
shell radius
stolon axis
cone mantle
E
intersection of cone mantle with cone base
B
exoskeletal realm
endoskeletal realm
cone radius
apertural face
cone mantel line
chamber suture
F
crosswise-oblique stolon axes
G
C
reticular zone
cone mantle
chamber suture
radial zone

◀ **Figure 80:** Stolon planes and foramenal axes in discoidal-annular and conical-uniserial shells. Schematic, not to scale.
A: Discoidal shell with a broadening periphery. Green and blue stolon planes are added step by step to the equatorial plane (E) as the shell margin thickens during ontogeny. The sector cut from the disc is cut in its turn in a transverse direction. **B:** A cone composed of a single series of discoidal chambers of which the marginal and axial areas are differentiated by colour. Note the distribution of the marginal area, the emplacement of the exoskeleton, and of the axial area housing the endoskeleton, in axial, horizontal (basal) and transverse sections. The axis of the shell is indicated by a vertical arrow. The surface of the cone is called the **cone mantle**, its horizontal termination is the **cone base**. A vertical line on the slanting surface of the cone is called a **cone mantle line**. The **cone radius** is indicated by a double arrow. **C:** The stolon axes are distributed on cone mantles in conical- uniserial foraminifera. If the cones increase their radial dimension markedly during growth, additional cone mantles are added in order to maintain the radial distances between the cone mantles relatively constant. This addition of cone mantles disturbes the regularity of the endoskeletal structures. In the models D-G, the addition of cone mantles during ontogeny is not taken into account. **D-G:** arrangement of stolon axes on cone mantles in the so-called radial zone of the cone (Fig. 20) is in accordance with the four basic patterns that govern discoidal structures. In conical shells, however, the stolon planes are replaced by cone mantles. As the cone increases in radius during growth, new stolon axes are intercalated in the cone mantles (arrows). **D:** stolon axes in the cone mantles alternate in radial position as a mantle is added, *e.g. Dictyoconus*. **E:** arrangement of stolon axes on cone mantle lines aligned on a cone radius. **F:** crosswise-oblique arrangement of stolon axes alternating in radial position on successive cone mantles. **G:** crosswise-oblique arrangement of stolon axes in line on a shell radius on subsequent cone mantles. This structure is a characteristic of *Orbitolina* (Fig. 71).

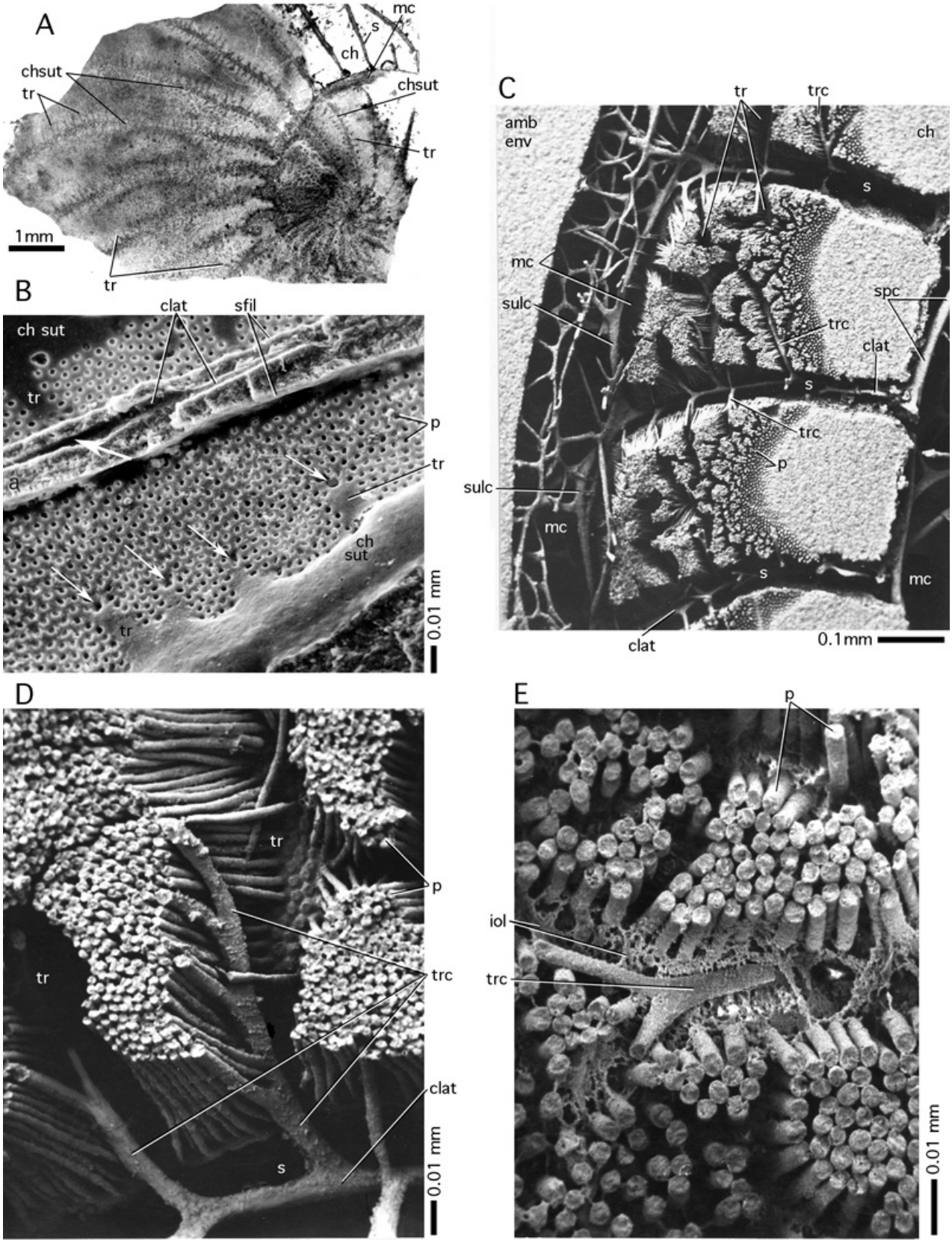
A
mc
s
ch
chsut
tr
chsut
tr
1mm
tr
B
clat
sfil
ch sut
tr
p
tr
a
ch
sut
tr
0.01 mm
C
tr
trc
amb
env
ch
s
mc
sulc
spc
trc
clat
s
trc
p
sulc
mc
s
mc
clat
0.1mm
D
tr
p
tr
trc
clat
s
0.01 mm
E
p
iol
trc
0.01 mm

◀ **Figure 81:** Trabeculae.
A: trabecules in a totally evolute nummulite, *Nummulites giganteus* (MAYER-EYMAR). Crimea. Lower Eocene (Cuisian). Transmitted light micrograph of a section tangential to the lateral chamber walls. **B-D:** unfilled shells of *Nummulites planulatus* (LAMARCK) from Bos d'Arros, Gan, Southwestern France, Cuisian. **B:** lateral surface of the shell with a part of a septal suture between alar prolongations and their extensions, the trabeculae. The white arrows indicate the orifices of the trabecular canals. The lateral surface is overgrown by the next whorl that has been broken away above the basal suture of a septum of an alar prolongation leaving a linear mark called septal filament. At the base of the septum of an alar prolongation there is a single intraseptal canal running the lenght of the alar prolongation. Where such a canal crosses a trabecular orifice (arrow), a passage may be created by partial resorption of the wall. This passage connects canal cavities of two successive whorls. SEM graph. **C:** epoxy-resin cast of shell cavities cut in an approximately equatorial direction showing two complete chambers with their marginal cord. Note the "grooves" in the porous wall created by the trabecular canals. SEM graph. **D:** detail of C showing the deviation of the pores in order to admit a trabecular canal. **E:** trabecular canal in *Nummulites partschi* DE LA HARPE from Bos d'Arros, Gan. Cuisian. Epoxy resin cast. The preservation of the interlamellar organic lining as a cavity in the shell permits the oblique path of the trabecular canal to be followed through subsequent lamellae.
Abreviations: **amb env:** ambient environment appearing in a cast of cavities as solid mass; **ch:** chamber lumen; **chsut:** chamber suture; **clat:** lateral intraseptal canals in the chamber and in the alar prolongations; **iol:** interlamellar organic layer; **mc:** marginal cord; **p:** pores; **sfil:** septal filament; **spc:** spiral canal; **sulc:** sulcus; **tr:** trabecule; **trc:** trabecular canal.

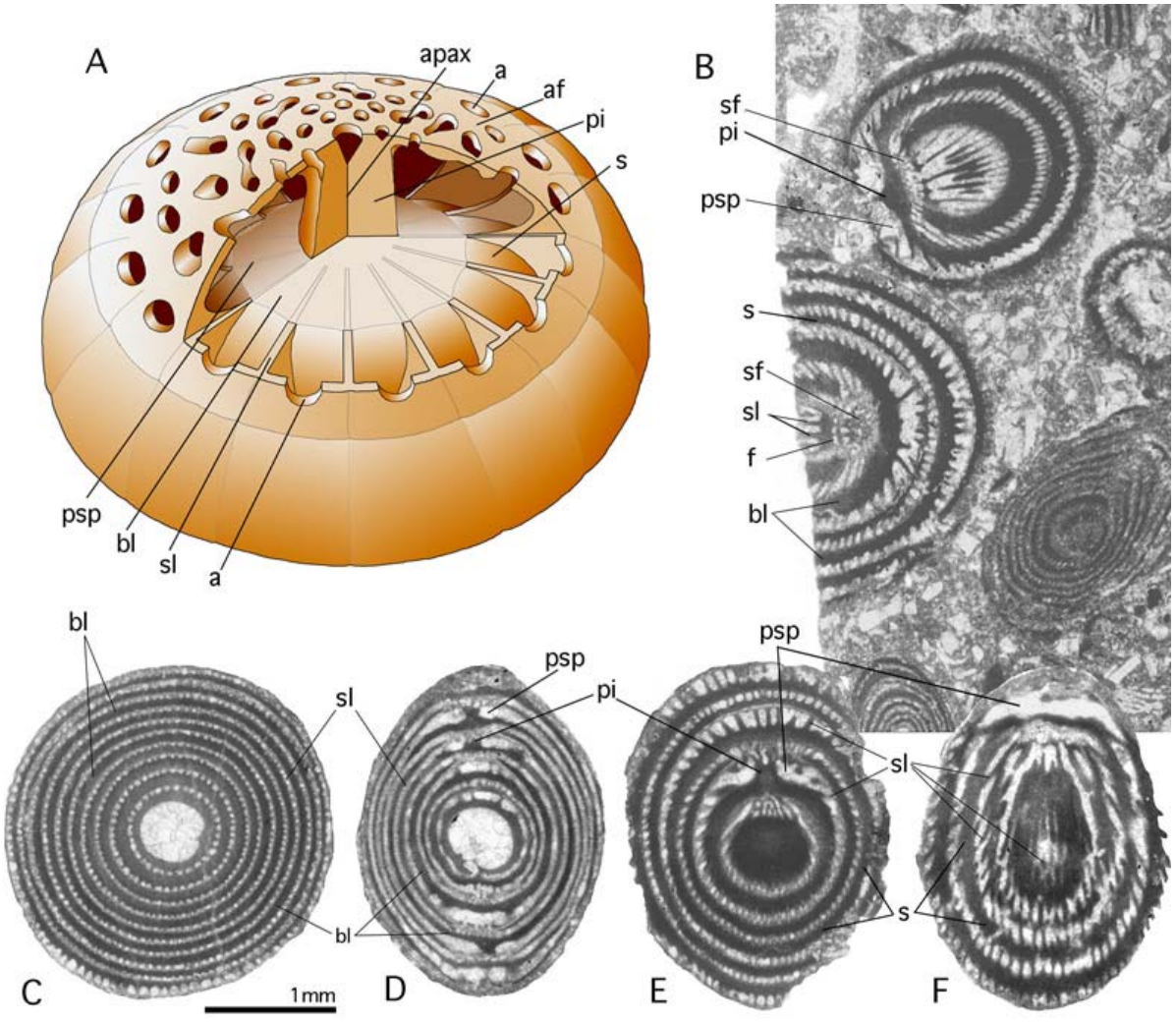

Figure 82: Trematophores.
A: stereograph of the trematophore of *Lacazinella* supported by a single residual pillar in axial position. Schema, not to scale. **B-F:** *Lacazinella wichmanni* (SCHLUMBERGER) from the Vogelkop, New Guinea. Middle-Upper Eocene. Transmitted light micrographs. All specimens are megalospheric. **B:** sections tangential to a septal face. **C:** a section perpendicular to the apertural axis reveals the concentric growth of the chambers from their beginning. **D:** section in the apertural axis. Note the alternation of the trematophore on opposite poles of the shell in successive chambers. **E:** oblique section cutting the apertural axis in a pillar supporting the trematophore. **F:** oblique section not cutting the apertural axis within the shell. Note the interruption of the septula below the equatorial roof of the chambers.
a: aperture; **af:** apertural face; **apax:** apertural axis; **bl:** basal layer; **f:** foramen; **pi:** pillar; **psp:** preseptal space; **s:** septum by transformation of the outer chamber wall that is totally covered by a new concentric chamber; **sf:** septal face; **sl:** septulum.

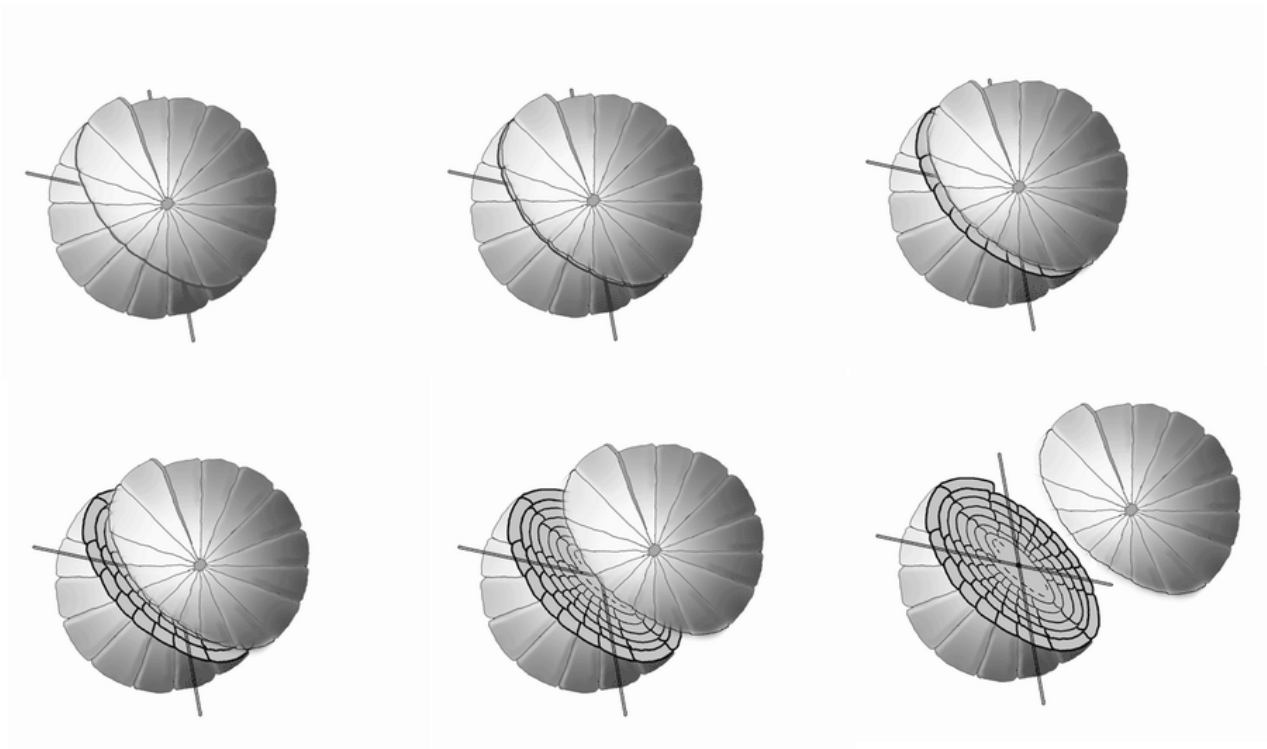

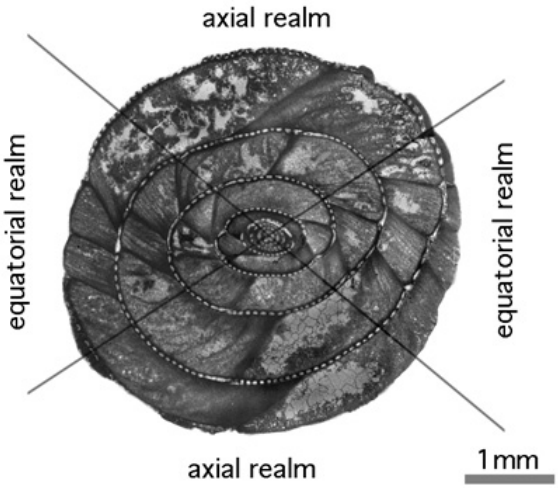

Figure 83: Model in polar view and a globular *Alveolina* (Middle (?) Eocene of Pakistan) cut in a similar direction. Note the shortened distance between the septa in the equatorial and the lengthened distance in the axial realm. In oblique sections of globular to elongate involute planispiral shells the structure of the chambers in opposite sectors of the section approaches more or less closely in appearance that of either an equatorial or an axial section depending on the location and angle of the cut with respect to the septa.

List of the illustrated taxa